Assessing the effects of modeling the spectrum of clinical symptoms on the dynamics and control of Ebola

Joan Ponce[1]*, Yiqiang Zheng[1]†, Guang Lin[1,2]‡, Zhilan Feng[1]§
[1]Department of Mathematics, Purdue University, West Lafayette, IN 47907
[2]School of Mechanical Engineering, Purdue University, West Lafayette, IN 47907

October 24, 2018

Abstract

Mathematical modelers have attempted to capture the dynamics of Ebola transmission and to evaluate the effectiveness of control measures, as well as to make predictions about ongoing outbreaks. Many of their models consider only infections with typical symptoms, but Ebola presents clinically in a more complicated way. Even the most common symptom, fever, is not experienced by 13% of patients. This suggests that infected individuals could be asymptomatic or have moderately symptomatic infections as reported during previous Ebola outbreaks. To account crudely for the spectrum of clinical symptoms that characterizes Ebola infection, we developed a model including moderate and severe symptoms. Our model captures the dynamics of the recent outbreak of Ebola in Liberia. Our estimate of the basic reproduction number is 1.83 (CI: 1.72, 1.86), consistent with the WHO response team's estimate using early outbreak case data. We also estimate the effectiveness of interventions using observations before and after their introduction. As the final epidemic size is linked to the timing of interventions in an exponential fashion, a simple empirical formula is provided to guide policy-making. It suggests that early implementation could significantly decrease final size. We also compare our model to one with typical symptoms by excluding moderate ones. The model with only typical symptoms overestimates the basic reproduction number and effectiveness of control measures, and exaggerates changes in peak size attributable to the timing of interventions. In addition, uncertainty about how moderate symptoms affect the basic reproduction number is considered, and PRCC (Partial rank correlation coefficient) is used to analyze the global sensitivity of relevant parameters. Possible control strategies are evaluated through numerical simulations and sensitivity analysis, indicating that simultaneously strengthening contact-tracing and effectiveness of isolation in hospital would be most effective. In this study, we show that asymptomatic Ebola infections may have implications for policy-making.

*Email: ponce0@purdue.edu
†Email: zheng30@purdue.edu
‡Corresponding author, email: guanglin@purdue.edu
§Email:fengz@purdue.edu

1 Introduction

The 2014-15 Ebola outbreak in West Africa, which presented a serious threat to global public health, was declared a "public health emergency of international concern" by the WHO on August 8, 2014 [3]. The Ebola virus is transmitted among humans through close contact with bodily fluids of infected ill and dead persons, including blood, secretions, etc. [30]. Symptoms of Ebola infection vary widely, but commonly include fever, fatigue, loss of appetite, vomiting, diarrhea, and headache, as well as hemorrhagic symptoms [30]. For the 2014-15 West African Ebola outbreak, 87% of infected individuals exhibited fever, the most commonly reported symptom. And some hemorrhagic symptoms are rarely reported (<5.7%) [30]. This suggests that infected individuals experience a range of symptoms from mild to severe. Asymptomatic infections are quite possible, as shown in previous Ebola outbreaks [15, 18].

In the past year, two studies analyzed minimally symptomatic and asymptomatic ebola in the 2014-15 outbreak. Bower et al. tested 933 people in Kerry town, Sierra Leone, and found evidence of asymptomatic ebola in roughly 2.6% of the population studied. Additionally, 12% reported some symptoms and although they were undiagnosed, tested positive for Ebola antibodies [9]. A slightly smaller survey by Richardson et al. on minimally symptomatic Ebola reported that up to 25% of Ebola infections may have been minimally symptomatic [22], which is consistent with previous outbreaks estimates [15, 18].

Some of the spectrum of Ebola symptoms might be explained by immunological responses to infection [6, 31, 32]. Following the infection of some naive individuals, Ebola virus could evade the innate immune response by interfering with or disabling the detection and signaling functions of immune cells, for instance, dendritic cells and macrophages. This evasion could lead to systemic viral replication and increase the chance of disease-induced death due to multiple organ failure. For infected people whose innate responses to infection are successful, however, the initial replication of Ebola virus may be limited or even contained, resulting in few or mild symptoms [18]. The difference in immunological responses may be related to host genetics and/or partial immunity due to previous infection with a related virus. Host genetic studies [11] show that genetic background determines susceptibility and resistance to many infectious diseases, including the strain Ebola virus recently circulating in West Africa [21]. Thus, host genetics may determine if individuals are resistant or susceptible to severe hemorrhagic fever [25].

Many mathematical models have been applied to the 2014-15 Ebola outbreak in West Africa to estimate the basic reproduction number and evaluate control measures [5, 7, 10, 16, 17, 19, 23, 28]. However, with few exceptions [8, 20], these studies do not consider asymptomatic or moderately symptomatic infections. Using a simple model without post-mortem or nosocomial transmission, Bellan et al. [8] showed that models without asymptomatic infection overestimate epidemic size. Pandey et al. [20] included asymptomatic infection in their model, but studied only its influence on epidemic sizes with different possible control measures. In addition, those authors did not study moderately symptomatic individuals, who might have reduced infectivity. The consequences of including moderately symptomatic individuals in the model warrants detailed study.

To account crudely for the spectrum of clinical symptoms that characterizes Ebola infection, we model moderate and severe infections. We augment Model II in [13] by adding moderately symptomatic to susceptible, exposed, infectious, hospitalized and deceased (not buried yet) and recovered compartments. In this model, the underlying transitions of infectious persons to hospitalization and disease progression are assumed to be independent stochastic processes (see Section 2 for a more detailed description). A

Gamma distribution is adopted for a more realistic, yet mathematically tractable, infectious period. If Ebola virus replicates, but is contained by a strong innate immune response, the resulting moderate symptoms are captured by moving people from the exposed compartment to the moderately infectious compartment. Based on their viral load, those moderately symptomatic individuals from the exposed class probably are infectious, but less so than those with severe symptoms.

These moderately symptomatic people are important in estimating basic reproduction number and evaluating control effectiveness. For example, early outbreak data from Liberia are used to estimate the basic reproduction number (there were limited effects of control measures before the middle of September, 2014 [20, 30]) as 1.83 from the model with 30% moderate infections, which is consistent with the WHO estimate via a different approach. If moderate symptoms are disabled, however, the estimated reproduction number is 1.94, which is 6% higher. This shows that models without considering moderate infections might overestimate the basic reproduction number. In addition, the model without moderately symptomatic infections overestimates the reduction in transmission rates in the community, hospitals and after death due to international interventions. This implies that credit given to control measures may actually be due to moderately symptomatic infections.

This paper is organized as follows: Section 2 elaborates the model, in which infections with moderate symptoms are explicitly incorporated, and the stage durations for both severe and moderate infections follow gamma distributions. The basic and control reproduction numbers are derived in Section 3. Model calibration to the Liberia outbreak and parameter estimation are presented in Section 4. In Section 5, various control strategies are evaluated and models with and without considering minimally symptomatic individuals are compared. Section 6 is devoted to sensitivity and uncertainty analyses for several outcomes including the reproduction number, peak incidence, and final epidemic size. Discussion of the results is included in Section 7.

2 A new model with severe and moderate infections

The objective of this paper is to enhance our understanding of the effects of including minimally symptomatic individuals on Ebola modeling. A compartmental model is developed by including a compartment for infected individuals with moderate symptoms. One of the important control measures for Ebola is isolation, which will be considered in our model as well. It has been demonstrated that, when control measures such as isolation are included in epidemiological models, one must consider disease sojourns that are more realistic than exponential distributions to avoid biased evaluations of disease control and prevention programs [14]. It has also been pointed out in [13] that, depending on the underlying assumptions on the epidemiological processes (e.g., recovery, hospitalization, disease induced death, etc.), the transition diagram between epidemiological classes can be very different, leading to significantly different model equations (see Models I, II and III and the corresponding transition diagrams in [13]). In this paper, we adopt the same underlying assumption as for Model II in [13], which assumes that, from individuals with severe infections, the transitions to hospitalization and disease progression (recovery or death) are independent. Intuitively, the waiting times of these transitions are measured by two independent clocks. If the hospitalization clock rings before recovery or death, the clock of disease progression continues to run until either recovery or death. If the disease progression clock rings before hospitalization, the individual dies with probability f and recovers with probability $1 - f$. More detailed explanations can be found in

[13] including the reduction of this model from a system of integro-differential equations (with arbitrary stage durations) to a system of ordinary differential equations (ODEs) when waiting times follow Gamma distributions. When disease progression follows a Gamma distribution with shape parameter $n \geq 1$ and rate parameter γ, the hospitalization process follows an exponential distribution with parameter χ (a gamma distribution with shape parameter equal to 1) and disease progression for the moderate infections follows a Gamma distribution with shape parameter $m \geq 1$ and rate parameter γ_a; the transition diagram is depicted in Figure 1.

The total population is divided into the following epidemiological classes: susceptible S, latent (exposed) E, infectious with severe symptoms I_j, $j = 1, 2, \ldots, n$, infectious with moderate symptoms J_k, $j = 1, 2, \cdots, m$, hospitalized H_j, $j = 1, 2, \cdots, n$, disease-induced death and not safely buried D, and recovered R. The total population is $N = S+E+I+J+H+R$, where $I = \sum_{j=1}^{n} I_j(t)$, and $H = \sum_{j=1}^{n} H_j(t)$, and $J = \sum_{k=1}^{m} J_k(t)$. A diagram for transitions between classes is shown in Figure 1.

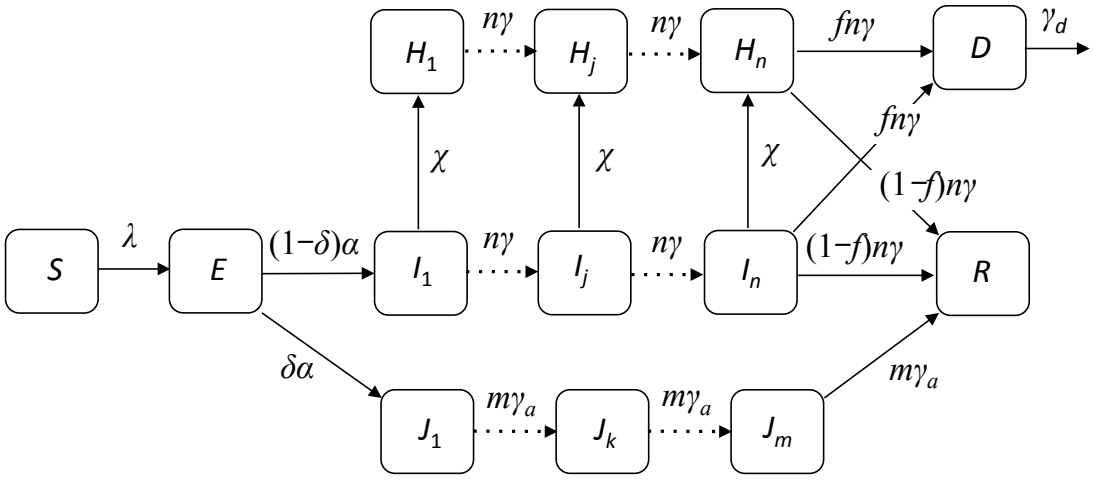

Figure 1: Transition diagram between epidemiological classes under the assumption of Gamma distributed infectious stages for severe infections (I_j, $j = 1, 2, \cdots, n$) and moderate infections (J_k, $k = 1, 2, \cdots, m$) with shape parameters n and m, respectively. The mean infectious periods of these two types of infections are $1/\gamma$ and $1/\gamma_a$, and the mean duration from the time of death to burial is $1/\gamma_d$. The *per-capita* rate of hospitalization for individuals with severe infections is χ; this is the rate at which individuals in the I_j compartment enter the H_j compartment. The proportion of deaths for severe infections is f.

For new infections, depending on the outcome of viral replication and host immunological response, individuals could be mildly infectious with moderate symptoms (with a fraction δ) or fully infectious with severe symptoms (with a fraction $1 - \delta$). The force of infection, denoted by $\lambda(t)$, is given by

$$\lambda(t) = \frac{\beta_I \big[I(t) + \varepsilon J(t)\big] + \beta_H H(t) + \beta_D D(t)}{N(t)},$$

where β_I, β_H, and β_D are transmission rates in the community, hospital and at funerals (deceased but not yet safely buried), respectively, and ε is a factor $(0 \leq \epsilon \leq 0.2)$ representing the reduced infectivity of individuals with moderate symptoms (or the ratio of infectivities of moderate to severe infections). The infectious periods of moderate and severe symptoms are assumed to follow Gamma distributions with

shape parameters being m and n, and mean infectious periods being $1/\gamma_a$ and $1/\gamma$, respectively. This is equivalent to considering m and n sub-stages with transition rates from each sub-stage to the next equal to $m\gamma_a$ and $n\gamma$ (see Figure 1). Individuals with severe infections may be hospitalized at rate χ while being at each of the n sub-stages. Deaths due to infection only occurs at the last sub-stage of severe infections. Because this is an epidemic model for a single outbreak, demographic processes (births and natural deaths) are ignored.

The model consists of the following differential equations:

$$\begin{aligned}
\frac{dS}{dt} &= -\lambda(t)S, \\
\frac{dE}{dt} &= \lambda(t)S - \alpha E, \\
\frac{dI_1}{dt} &= (1-\delta)\alpha E - (n\gamma + \chi)I_1, \\
\frac{dI_j}{dt} &= n\gamma I_{j-1} - (n\gamma + \chi)I_j, \quad j = 2, \ldots, n, \\
\frac{dH_1}{dt} &= \chi I_1 - n\gamma H_1, \\
\frac{dH_j}{dt} &= \chi I_j + n\gamma H_{j-1} - n\gamma H_j, \quad j = 2, \ldots, n, \\
\frac{dJ_1}{dt} &= \delta\alpha E - m\gamma_a J_1, \\
\frac{dJ_k}{dt} &= m\gamma_a J_{k-1} - m\gamma_a J_k, \quad k = 2, \ldots, m, \\
\frac{dD}{dt} &= fn\gamma I_n + fn\gamma H_n - \gamma_d D, \\
\frac{dR}{dt} &= (1-f)n\gamma I_n + (1-f)n\gamma H_n + m\gamma_a J_m,
\end{aligned} \tag{1}$$

where δ is the fraction of infections with moderate symptoms; $1/\gamma$ and $1/\gamma_a$ are the average infectious periods for infections with severe and moderate symptoms; $1/\alpha$ is the latent period; χ is rate at which individuals with severe symptoms are hospitalized; and f is the fraction of severe infections resulting in death. As discussed in [13], for this model the parameter γ can be chosen to be the weighted average of the interval from disease onset to recovery, $1/\gamma_{IR}$, and from onset to death, $1/\gamma_{ID}$, in the following form:

$$\frac{1}{\gamma} = (1-f)\frac{1}{\gamma_{IR}} + f\frac{1}{\gamma_{ID}}. \tag{2}$$

All parameters with their definitions and the ranges of their values are also listed in Table 1. The WHO Ebola Response Team published estimates for the 2014-15 Ebola outbreak in West African [30]. Recent studies estimated the reproduction number by fitting models to the symptom onset date during the initial stage of this outbreak [5, 16], and estimated parameters and evaluated interventions by calibrating models using this outbreak data [20, 23]. Similar studies for previous outbreaks include [12, 27] and [17] which focused on estimates from the 1995 Congo and 2000 Uganda outbreaks, respectively.

Table 1: Definition of the parameters in model (1), and the ranges of their values used in numerical simulations and sensitivity analysis.

Symbol	Definition	Value (Range)	References
β_I	Community transmission rate	0.319 (0.3, 0.33)	estimated
β_H	Hospital transmission rate	0.6 (0.55, 0.65)β_I	[16]
β_D	Traditional burial transmission rate	1.2 (1, 1.25)β_I	[20, 24]
ε	Ratio of infectivities of moderate to severe infections	0.1 (0, 0.2)	assumed
$1/\chi$	Mean time from disease onset to hospitalization	4.9 (4.8, 5.3) days	[17, 27, 30]
$1/\gamma_{ID}$	Mean time from disease onset to death	7.9 (7.5, 8.5)days	[17, 27]
$1/\gamma_{IR}$	Mean time from disease onset to recovery	9 (8.5, 9.5)days	[20]
$1/\gamma$	Mean of the Gamma distribution for severe infection	$= \frac{1-f}{\gamma_{IR}} + \frac{f}{\gamma_{ID}}$	[13]
$1/\gamma_a$	Mean of the Gamma distribution for moderate infection	3.1 (3, 7) days	assumed
$1/\gamma_d$	Mean time from deceased to buried	2.02 (1.5, 2.5) days	[17, 20, 27]
$1/\alpha$	Latent period	9.5 (9, 12)days	[12, 20, 30]
δ	Proportion of infections with moderate symptoms	0.3 (0.1, 0.42)	[8]
f	Proportion of disease death for severe infections	0.6966 (0.69, 0.73)	[12, 30]

3 Derivation of the basic and control reproduction numbers

The basic (control) reproduction number, denoted by $\mathcal{R}_0$ ($\mathcal{R}_c$) are the average numbers of secondary infections caused by an infected individual while infectious in a susceptible population in the absence (presence) of disease control. Instead of using the usual method of next generation matrix to derive the reproduction number, we use a more intuitive approach based on the underlying stochastic processes.

For an infectious person in the I compartment (i.e., with severe symptoms), let T_P and T_L denote the stochastic waiting times for disease progression and hospitalization, respectively, and let $\mathbb{E}(T_P)$ and $\mathbb{E}(T_L)$ denote the expectations of T_P and T_L. Then $\mathbb{E}(min\{T_P, T_L\})$ is the expected time before leaving I due to either disease progression or hospitalization, and $\mathbb{E}(T_P) - \mathbb{E}(min\{T_P, T_L\})$ is the expected time in the H compartment. Moderately symptomatic individuals will not be hospitalized so have only a waiting time for onset to recovery, which we denote by T_a, and the expected duration is $\mathbb{E}(T_a)$. Then the control reproduction number is the weighted average of the reproduction numbers with severe and moderate infections, which can be written as:

$$\mathcal{R}_c = (1-\delta)\mathcal{R}_{c1} + \delta\mathcal{R}_{c2}, \tag{3}$$

where $\mathcal{R}_{c1}$ and $\mathcal{R}_{c2}$ represent the secondary infections produced by an individual with severe and moderate symptoms, respectively, given by

$$\begin{aligned} \mathcal{R}_{c1} &= \beta_I \mathbb{E}(min\{T_P, T_L\}) + \beta_H \left[\mathbb{E}(T_P) - \mathbb{E}(min\{T_P, T_L\})\right] + \beta_D \tfrac{f}{\gamma_d}, \\ \mathcal{R}_{c2} &= \varepsilon\beta_I \mathbb{E}(T_a). \end{aligned} \tag{4}$$

It is clear that each term in $\mathcal{R}_{ci}$ $(i = 1, 2)$ is a product of transmission rate with the corresponding expected durations.

To compute the expectations under Gamma distributed sojourns, note that the waiting times T_P, T_L

and T_a have the following survival functions:

$$G^n_{n\gamma}(t) = \sum_{j=1}^{n} \frac{(n\gamma t)^{j-1} e^{-n\gamma t}}{(j-1)!}, \quad G^1_{\chi} = e^{-\chi t}, \quad G^m_{m\gamma_a}(t) = \sum_{j=1}^{n} \frac{(m\gamma_a t)^{j-1} e^{-m\gamma_a t}}{(j-1)!}.$$

It follows that $\mathbb{E}(T_P) = 1/\gamma$, $\mathbb{E}(T_L) = 1/\chi$, $\mathbb{E}(T_a) = 1/\gamma_a$,

$$\begin{aligned} \mathbb{E}(min\{T_P, T_L\}) &= \int_0^\infty \sum_{j=1}^{n} \frac{(n\gamma t)^{j-1} e^{-n\gamma t}}{(j-1)!} e^{-\chi t} dt = \sum_{j=1}^{n} \int_0^\infty \frac{(n\gamma t)^{j-1} e^{-(n\gamma+\chi)t}}{(j-1)!} dt \\ &= \frac{1}{n\gamma+\chi} \sum_{j=1}^{n} \left(\frac{n\gamma}{n\gamma+\chi}\right)^{j-1} = \frac{1}{\chi}\left[1 - \left(\frac{n\gamma}{n\gamma+\chi}\right)^n\right], \end{aligned}$$

and

$$\mathbb{E}(T_P) - \mathbb{E}(min\{T_P, T_L\}) = \frac{1}{\gamma} - \frac{1}{\chi}\left[1 - \left(\frac{n\gamma}{n\gamma+\chi}\right)^n\right].$$

Therefore, from (3) and (4) we have

$$\mathcal{R}_c = (1-\delta)\left\{\beta_I \frac{1}{\chi}\left[1 - \left(\frac{n\gamma}{n\gamma+\chi}\right)^n\right] + \beta_H\left(\frac{1}{\gamma} - \frac{1}{\chi}\left[1 - \left(\frac{n\gamma}{n\gamma+\chi}\right)^n\right]\right) + \beta_D \frac{f}{\gamma_d}\right\} + \frac{\delta\varepsilon\beta_I}{\gamma_a}. \quad (5)$$

It can be verified that the expression for $\mathcal{R}_c$ given in (5) is equivalent to that obtained using the next generation matrix method. The effects of disease control measures are represented by reduced transmission rates β_i $(i = I, H, D)$ and the duration from death to burial $1/\gamma_d$, and an increased rate of hospitalization χ. In the absence of changes of these parameter values, formula (5) provides an expression for the basic reproduction number $\mathcal{R}_0$.

Denote the four components of $\mathcal{R}_c$ associated with I, H, D, and J by $\mathcal{R}^I_c$, $\mathcal{R}^H_c$, $\mathcal{R}^D_c$, and $\mathcal{R}^J_c$, respectively. Then the expression in (5) can also be written as

$$\mathcal{R}_c = \mathcal{R}^I_c + \mathcal{R}^H_c + \mathcal{R}^D_c + \mathcal{R}^J_c,$$

where

$$\begin{aligned} \mathcal{R}^I_c &= (1-\delta)\beta_I \frac{1}{\chi}\left[1 - \left(\frac{n\gamma}{n\gamma+\chi}\right)^n\right], \\ \mathcal{R}^H_c &= (1-\delta)\beta_H\left(\frac{1}{\gamma} - \frac{1}{\chi}\left[1 - \left(\frac{n\gamma}{n\gamma+\chi}\right)^n\right]\right), \\ \mathcal{R}^D_c &= (1-\delta)\beta_D \frac{f}{\gamma_d}, \\ \mathcal{R}^J_c &= \frac{\delta\varepsilon\beta_I}{\gamma_a}. \end{aligned} \quad (6)$$

These expressions in (6) can be helpful for examining how various factors may affect $\mathcal{R}_c$.

Remark: In the case when moderate infections are not considered, i.e., $\delta = 0$, the reproduction number given in (5) becomes $\mathcal{R}_c = \mathcal{R}_{c1}$ (see (4)), which is exactly the same as the reproduction number for Model II in [13]. This allows us to compare the models with and without moderate infections.

4 Data fitting and parameter estimation

We will use the situation in Liberia based on the WHO situation reports [2] to calibrate the model equations in (1). For demonstration purposes, we consider the model for the case of $n = 2$ and $m = 1$. The data corresponding to the initial phase of exponential growth is used to estimate the transmission parameters β_i $(i = I, H, D)$, which are then used to determine $\mathcal{R}_0$ using formula (5). By fitting the model to reports after control started we can estimate the reductions in the transmission rates and the control reproduction number, $\mathcal{R}_c$, which then allows us to evaluate alternative control scenarios.

4.1 Estimation of transmission rates and the reproduction number

Data from the Liberia outbreak were obtained through the CDC's website [1], which are extracted from WHO situation reports [2]. Though there were some local efforts to curtail the outbreak from the middle of August 2014, their effects were not significant [20]. Observations before September 14, 2014 are suitable for estimating the reproduction number because interventions had not yet altered the epidemic curve [30]. To have an accurate estimate, we used the data from June 5, 2014 to September 14, 2014 to calibrate the models and estimate the reproduction number [20, 30].

The only parameters that we estimate are the transmission rates. For other parameters, we used the estimates obtained by the WHO Ebola Response Team [30] and others. The reported cases from Liberia are assumed to be Poisson samples from the model. We use R package bbmle for maximum likelihood estimation and the package deSolve for solving ODEs similar to [5]. These parameter values are listed in Table 1. This method firstly reassembles the data by combining predictions and residuals randomly. Second, the model is refitted to the reassembled data. Then confidence intervals are based on estimates of the refitted model.

We use the initial outbreak data (before September 14th) to estimate the transmission rates β_i $(i = I, H, D)$, from which we can obtain the corresponding estimate of $\mathcal{R}_0$ using formula (5). Furthermore, we fix β_H and β_D to be proportional to β_I with the proportions in certain ranges (see Table 1) so that the only transmission rate to be estimated is β_I.

We noticed that the curve fitting is particularly sensitive to the choice of the initial and end points of the selected time period for the exponential growth. To account for this issue, we performed an 8-fold cross validation, which was chosen to have similarly sized sub-samples. The analysis was performed on datasets with 25 points and 26 points, excluding and including the last point. The 25-point dataset with the minimum average error (RMSE) was chosen. In addition, because the fitted values will depend on the choice of the proportion of moderate infections δ, for which there is no commonly accepted value, we obtain estimates for several values of δ including the case of no moderate infections ($\delta = 0$). We use Bower et al.'s [9] estimate that 12% of infections are moderately symptomatic as a lower bound for the value δ and Bellan et al.'s [8] estimate of 40% as an upper bound. We considered four scenarios in this section: (a) $\delta = 0$; (b) $\delta = 0.15$; (c) $\delta = 0.3$; and (d) $\delta = 0.5$. The corresponding estimates of $\mathcal{R}_0$ are 1.94, 1.89, 1.83, and 1.71 (these values and the confidence intervals are also listed in Table 2). For these four cases (a)–(d), the fitted curves are illustrated in Figure 2. These fitted curves generates estimates of β_I values with corresponding confidence intervals equal to 0.244 (0.232,0.25), 0.275 (0.26, 0.28), 0.319 (0.309, 0.33), and 0.409 (0.39, 0.42), respectively. we used the Akaike information criterion (AIC) to

compare the models and evaluate which value of δ returns the best fit. The AIC estimates the relative quality of a statistical model for a given dataset by estimating the likelihood of a model to predict future values. The four different values of δ are analyzed as different models, the best model is the one with the minimum AIC ($\delta = 0.3$) among the candidate models.

Although the estimates of $\mathcal{R}_0$ in all cases of (a)–(d) are in the range of existing estimates [12, 27], the estimate in (c), i.e., $\mathcal{R}_0 = 1.83$ (95% CI, 1.76 to 1.88), is the most consistent with the estimate from WHO response team (obtained using other statistical methods). In addition, for case (c), we estimate that for community transmission, $\mathcal{R}_0^I = 0.78$ contributes the most to $\mathcal{R}_0$ at 42%. Contributions from other transmissions are $\mathcal{R}_0^H = 0.64$, $\mathcal{R}_0^D = 0.38$, and $\mathcal{R}_0^J = 0.03$, which consist of about 35%, 21%, and 1.6% of $\mathcal{R}_0$, respectively.

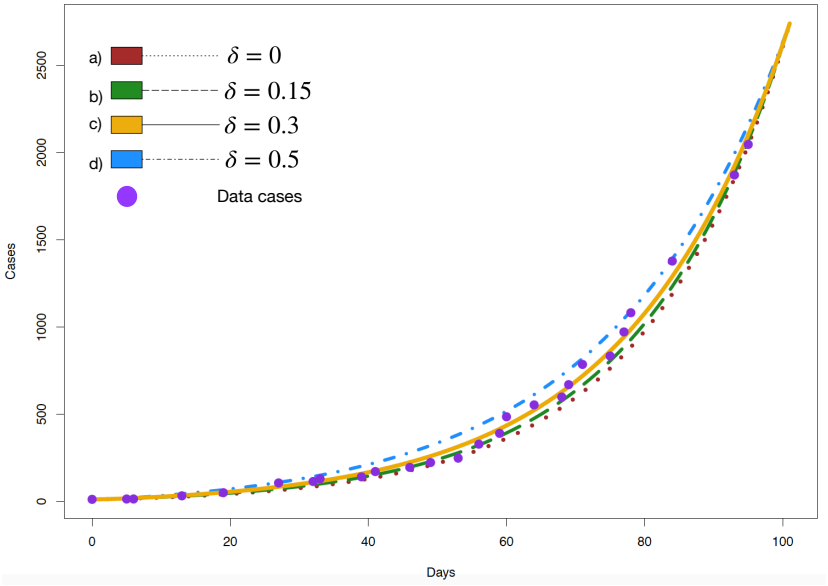

Figure 2: Fitting of model (1) to the 2014 Ebola reports before control (i.e., from June 5th to September 8th). The line plots correspond to different proportions of moderate infections: (a) $\delta = 0$, (b) $\delta = 0.15$, (c) $\delta = 0.3$ (d) $\delta = 0.5$. For the cases (a)–(d), the Akaike information criterion (AIC) are 325, 281, 267, and 341, respectively.

4.2 Estimates of the control parameters

In the countries with widespread and intense spreading, containment of the West African Ebola outbreak relied on non-pharmaceutical interventions due to the lack of effective medicines. These interventions include social mobilization, use of personal protective equipment (PPE) in healthcare facilities, safe and dignified burials, and contact-tracing and quarantine. Social mobilization activities include raising the population's awareness of mode of transmission, social distancing from infectious people, timely seeking of

Table 2: Estimates of $\mathcal{R}_0$ corresponding to the model fitting presented in Figure 2 for four cases with different proportions of moderate infections: (a) $\delta = 0$, (b) $\delta = 0.15$, (c) $\delta = 0.3$, (d) $\delta = 0.5$. Estimates of the components $\mathcal{R}_0^i$ $(i = I, H, D, J)$ of $\mathcal{R}_0$ are also provided.

Case	$\mathcal{R}_0$ (95% CI)	$\mathcal{R}_0^I$ (95% CI)	$\mathcal{R}_0^H$ (95% CI)	$\mathcal{R}_0^D$ (95% CI)	$\mathcal{R}_0^J$ (95% CI)
(a)	**1.94** (1.84, 2.01)	**0.84** (0.79, 0.86)	**0.69** (0.66, 0.71)	**0.41** (0.38, 0.43)	**0**
(b)	**1.89** (1.79, 1.93)	**0.81** (0.76, 0.82)	**0.67** (0.63, 0.68)	**0.4** (0.38, 0.42)	**0.012** (0.012, 0.013)
(c)	**1.83** (1.76, 1.88)	**0.78** (0.74, 0.8)	**0.64** (0.62, 0.66)	**0.38** (0.36, 0.39)	**0.03** (0.028, 0.031)
(d)	**1.71** (1.62, 1.75)	**0.71** (0.67, 0.73)	**0.59** (0.56, 0.60)	**0.35** (0.32, 0.36)	**0.064** (0.06, 0.065)

CI: Confidence Interval.

medical care and proper handling of deceased persons. Widely used, personal protective equipment (PPE) can lower infections in hospitals and other healthcare facilities. Safe and dignified burials conducted by trained teams can reduce transmission from deceased people. Contact-tracing helps to promptly identify and hospitalize suspected and isolate probable cases. All of these interventions are associated with one or multiple parameters in the model. A natural question is whether considering moderate symptoms in the model affects the estimated effectiveness of these interventions and to what extent ignoring this may contribute to biased evaluations.

Let t_c denote the time when intervention started in mid September, which for convenience is chosen to be 100 days from June 5th, 2014. To estimate the effect of control measures, we assume that the transmission rates for community (β_I), hospital (β_H), and funeral (β_D) are reduced by factors z_I, z_H, and z_D, respectively. That is, the transmission rates for $t > t_c$ will be $\beta_i(1-z_i)$, $i = I, H, D$. This change can be described by using piecewise-constant functions:

$$\beta_i(t) = \begin{cases} \beta_i & \text{for } t < t_c, \\ \beta_i(1 - z_i) & \text{for } t \geq t_c, \ i = I, H, D. \end{cases}$$

In addition, the time from onset to hospitalization $(1/\chi)$ is assumed to be reduced by 0.25, i.e., around 1.2 days earlier in hospitalization due to control [7].

The estimated values of reductions z_i in the transmission rates are shown in Table 3 for (i) $\delta = 0$ and (ii) $\delta = 0.3$. We observe that the reductions in case (i) is larger than that in (ii), implying that models that do not explicitly include moderate infections (case (i)) may overestimate the effectiveness of the control measures considered here.

Figure 3 shows the comparison between fitted model curves and reports for both the period before intervention ($t < t_c = 100$), which is the same as the curves shown in Figure 2, and after ($t > t_c = 100$). We observe that, when moderate infections are considered ($\delta > 0$), particularly for the case of $\delta = 0.3$ (see (ii)), this model fits the data much better than the model without considering moderate infections explicitly (see (i)). These results suggest again that considering moderate infections is necessary to estimate the effects of interventions for policy-making.

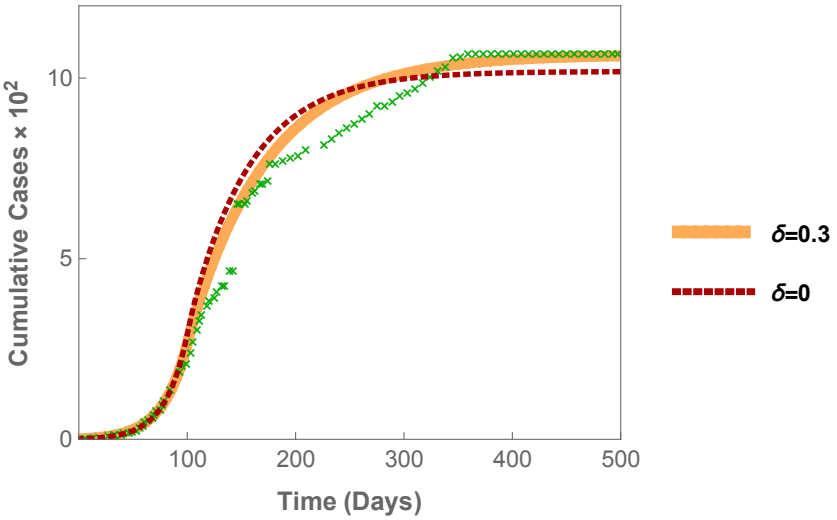

Figure 3: Fitting of the model (1) to the 2014 Ebola data for the period between June 5th, 2014 and October 8th, 2015. For $t < t_c = 100$, the fit is the same as in Figure 2, whereas the fit for $t > t_c = 100$ is used for estimating the control reduction parameters z_i $(i = I, H, D)$. The two cases are for δ values: (i) $\delta = 0$ and (ii) $\delta = 0.3$. The jump in cases between day 100 and day 200 is due to a catch up in monitoring and reporting in Liberia [4].

Table 3: Estimates of reductions (z_i, $i = I, H, D$) in transmission rates for four cases based on the proportion δ for moderate infections.

	Estimates (95% CI)	
Cases	(i) $\delta = 0$	(ii) $\delta = 0.3$
z_I	**0.987** (0.738, 1)	**0.83** (0.675, 0.945)
z_H	**0.514** (0.326, 0.652)	**0.49** (0.263, 0.51)
z_D	**0.23** (0, 0.527)	**0.217** (0, 0.259)

5 Evaluation of alternative control scenarios

Using the parameters estimated in the previous sections, we can experiment different scenarios for alternative control strategies. For example, if the reduction factors z_i $(i = I, H, D)$ were higher or lower than the estimated values, and/or if the time of control t_c started earlier or was delayed, how much that would have affected the disease outcomes in terms of final epidemic size, peak size, and duration. Apparently these evaluation results will be depend on the choice of other parameter values. Thus, we will also examine the sensitivity of the reproduction number $\mathcal{R}_c$ and other measures (final size, peak size, etc.) to various model parameters.

5.1 The effects of timing of interventions

The timing of interventions is critical for disease control. Let T denote the time of intervention, and consider $T = t_c = 100$ (days) as the baseline scenario. We first investigate earlier or delayed starting time and examine how they may affect the results of the outbreak using measures including final epidemic size, peak size, duration of outbreak, and total number of deaths.

In Figure 4, the epidemic curves and cumulative cases for various scenarios are plotted. Early intervention corresponds to the starting time $T = 86$ and 93 while late intervention corresponds to $T = 107$ and 114. This is for the case of 30% moderate infections (i.e., $\delta = 0.3$, the case (c) in Table 2). All other parameter are fixed at the same values, and z_i correspond to case (ii) in Table 3.

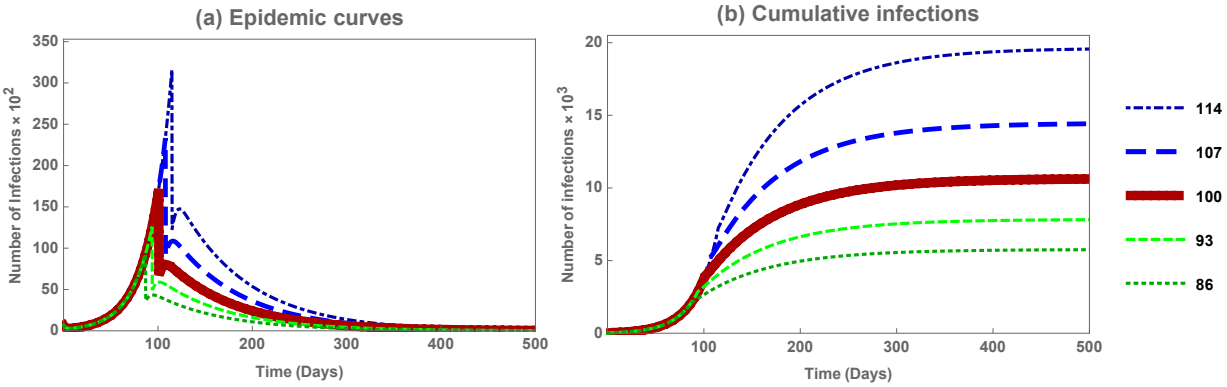

Figure 4: Plots of (a) epidemic curves and (b) cumulative infections for various times to intervention T: The baseline scenario $T = t_c = 100$ (thicker solid line), with one or two weeks early intervention $T = 86$ and 93 and one or two weeks delayed intervention $T = 107$ and 114.

We observe in Figure 4 that the difference in both peak sizes and final sizes are very large between early and late interventions. For example, the peak and final size values of early intervention are a half of the baseline scenario (the thick solid curve) values. Similarly, the peak and final sizes double when control is applied two weeks later than the hundredth day.

We can also compare models with different proportions of moderate infections, including the case when moderate infections are not explicitly considered (i.e., $\delta = 0$). Figure 5 shows simulation results corresponding to the same set of two δ values as before, to which we refer as two models. The cumulative and epidemic curves are shown in the top and bottom rows, respectively. The three columns are for (a) early intervention by one week ($T = 93$ days), (b) the baseline scenario $T = t_c = 100$ days), and (c) late intervention by one week ($T = 107$ days). It suggests again that the model with $\delta = 0$ overestimate the effects of early and delayed interventions. We observe in Figure 5 that, although the two models produce similar cumulative curves, they produce very different peak sizes for all three intervention times. Particularly, the peak size decreases with increasing δ, and the model without moderate infections ($\delta = 0$) produces the highest peak size, approximately 30% higher than the model with $\delta = 0.3$.

These differences between the two models are more transparent in Figure 6. The bar chart for peak sizes (a) shows that the reduction in peak sizes ($\mathcal{PS}$) with one week early intervention are 70 for $\delta = 0$ and 51 for $\delta = 0.3$ and the increase in peak sizes with one week late intervention are 88 for $\delta = 0$ and 62

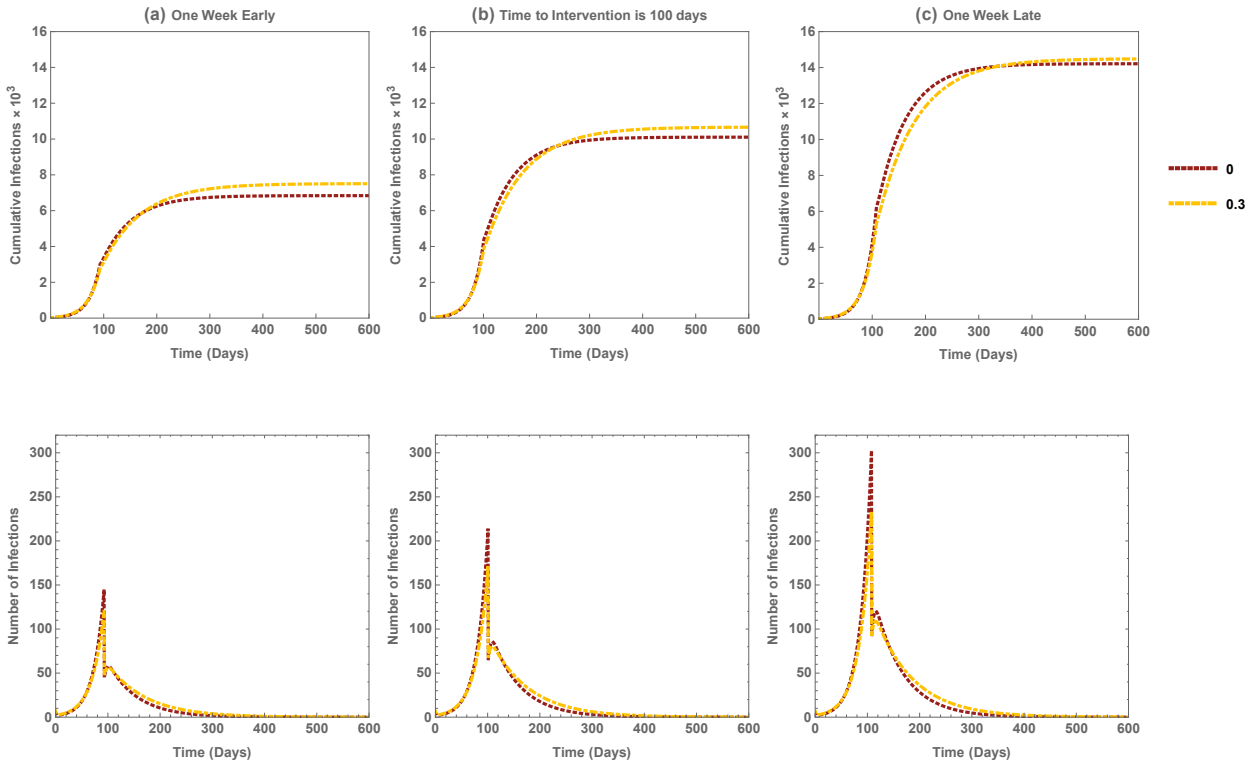

Figure 5: Comparison of models with different proportions (δ) of moderate infections and timing T of intervention: (a) $T = 93$ (one week early), (b) $T = t_c = 100$, and (c) $T = 107$ (one week late). The curves show cumulative infections for different δ values: $\delta = 0$ and 0.3.

for $\delta = 0.3$. The plot in (b) shows that changes in final sizes ($\mathcal{FS}$) generated by the two models do not differ significantly.

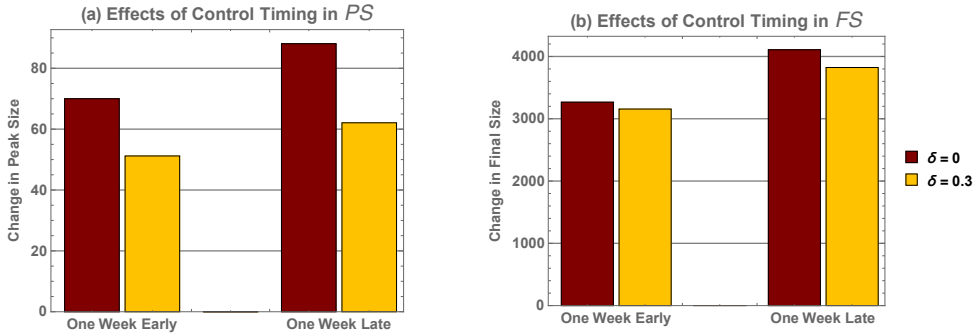

Figure 6: Changes by one week earlier or later than the baseline scenario (i.e., $T = t_c = 100$ days) in (a) peak size $\mathcal{PS}$ and (b) final size $\mathcal{FS}$ for $\delta = 0$ and $\delta = 0.3$. All parameter values are the same as in Figures 4 and 5.

It can be helpful to derive a functional relationship between the time to intervention and the final epidemic size. By fitting the regression line

$$FS(t) = FS(t_0)exp(k(t - t_0))$$

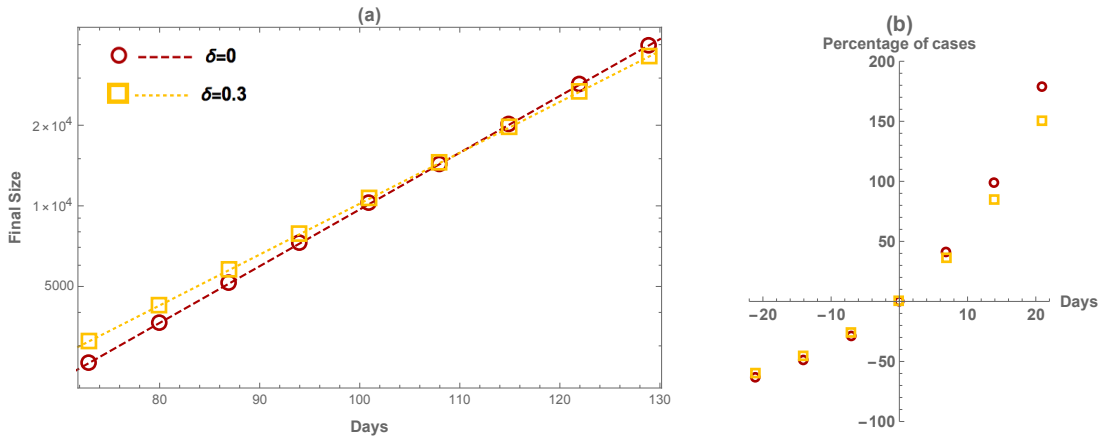

Figure 7: Percentage of change of final sizes as a function of time of intervention with respect to the baseline scenario ($T = t_c = 100$ days) corresponding to different fractions of moderate infections δ.

to the final size we obtained the values k=0.0488, 0.04375 for the cases of $\delta = 0$ and $\delta = 0.3$, respectively, as shown in Figure 7 (a). Figure 7 (b) is obtained using the formula $\frac{FS(t)-FS(t_c)}{FS(t_c)} * 100$. It shows the final size percentage increase or decrease as control is applied for different values of t. If control is applied a week early ($t = t_c - 7$) where $t_c = 100$, the percentage of cases per day is negative. That is, by applying control earlier we have prevented roughly 27% of cases. Similarly, if we apply control measures a week later than $t_c = 100$, the percentage is positive, i.e. the percentage increase is roughly 37%. We observe that the model without asymptomatic infections ($\delta = 0$) predicts a lower or higher final size for earlier or later interventions, respectively.

5.2 Effects of reducing transmission rates and stage durations

Evaluation of control strategies may also focus on the effect control measures on the control reproduction number $\mathcal{R}_c$. Joint effects of parameters on $\mathcal{R}_c$ can provide insights into the most effective factors in reducing $\mathcal{R}_c$. Some of these analyses are demonstrated in Figures 8 and 9.

Figure 8(a) shows that in the absence of reduction in β_H (i.e., $z_H = 0$), reducing $\mathcal{R}_c$ from 1.8 to 1.6 would require to reduce $1/\chi$ (time from onset to hospitalization) from 4.6 days to 1.5 days, which would be very difficult to do. On the other hand, if $1/\chi$ remains at 4 days, the reduction of $\mathcal{R}_c$ from 1.8 to 1.6 can be achieved by the reduction level at $z_H = 0.275$. Unless $1/\chi$ can be reduced to below 3 (days), it is impossible to reduce $\mathcal{R}_c$ to below 1 (see the thicker curve) by reducing β_H. In general, $\mathcal{R}_c$ can be effectively decreased by early hospitalization if the transmission rate in hospital is reduced. However, without the reduction of this transmission rate ($z_H = 0$), early hospitalization would not be effective in reducing $\mathcal{R}_c$. Early hospitalization might be achieved by contact-tracing, whereas the reduction in transmission rate β_H might be achieved by increasing the effectiveness of isolation in hospital and the use of personal protective equipment (PPE). A similar comparison between z_D and $1/\gamma_d$ (mean time from death to burial) can be made from Figure 8(b). For example, from the point where $z_D = 0.1$ and $1/\gamma_d = 2$ (days), reducing $1/\gamma_d$ by 0.5 days (i.e., from 2 to 1.5) can produce a similar reduction in $\mathcal{R}_c$ as improving the reduction level z_D from 0.1 to 0.3. It also shows that it is impossible to reduce $\mathcal{R}_c$ to

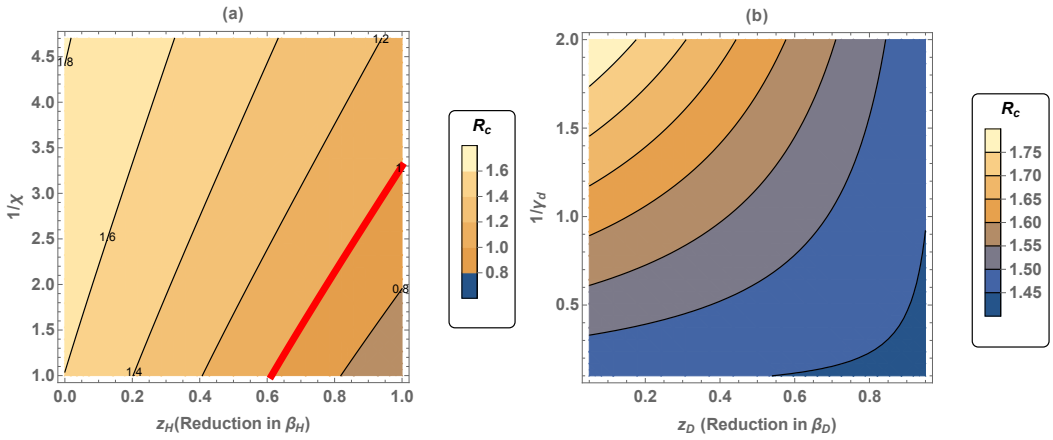

Figure 8: Contour plots of $\mathcal{R}_c$ in (a) the $(z_H, 1/\chi)$ plane and (b) the $(\beta_D, 1/\gamma_d)$ plane. See the text for detailed descriptions of the observations.

below 1 by only reducing $1/\chi$ and increasing z_D.

Figure 9 illustrates the comparisons of the effectiveness of combined reduction in transmission rates β_i $(i = I, H, D)$ for decreasing $\mathcal{R}_c$. The contour plots (a)–(d) illustrate the joint effect of reducing β_H and β_D under different levels of reduction in the community transmission rate β_I: $z_I = 0\%$, 10%, 20%, and 30%, respectively. We observe that, in all four cases, $\mathcal{R}_c$ is more sensitive to z_H than to z_D. An increase in z_H (higher reduction in β_H) is achievable by strictly implementing isolation and increasing the use of personal protective equipment by healthcare workers. We also observe that reducing $\mathcal{R}_c$ to below 1 is very difficult without reducing z_I, and that reductions in β_H and β_D have similar effects on reducing $\mathcal{R}_c$. In Figure 9(a), the vertical and horizontal dashed lines indicate that, to achieve $\mathcal{R}_c < 1$ (above the thick line) by reducing β_H and β_D alone (i.e., $z_I = 0$), the reduction in β_H must be higher than 70% ($z_H > 0.7$) and the reduction in β_D must be higher than 55% ($z_D > 0.55$). These threshold values of z_H and z_D decreases with increasing z_I, as illustrated in (b)–(d).

6 Uncertainty and sensitivity analyses

Uncertainty and sensitivity analyses are conducted for both the basic reproduction number $\mathcal{R}_0$ and epidemic outcomes including peak and final epidemic sizes.

6.1 Sensitivity analysis of $\mathcal{R}_0$

A sensitivity analysis of $\mathcal{R}_0$ provides important information regarding how uncertainty and variability of model parameters may affect model results and which parameters are most influential. The analysis is based on the Latin hypercube sampling method with 1000 points selected from assigned parameter ranges corresponding to the case of 30% moderate infections (see Table 1). The parameters considered in this analysis include transmission rates $(\beta_I, \beta_H, \beta_D)$, progression rates from onset to recovery or hospitalization (γ, γ_a, γ_d, χ), and factors related to moderate infections (δ and ε), and death fraction (f).

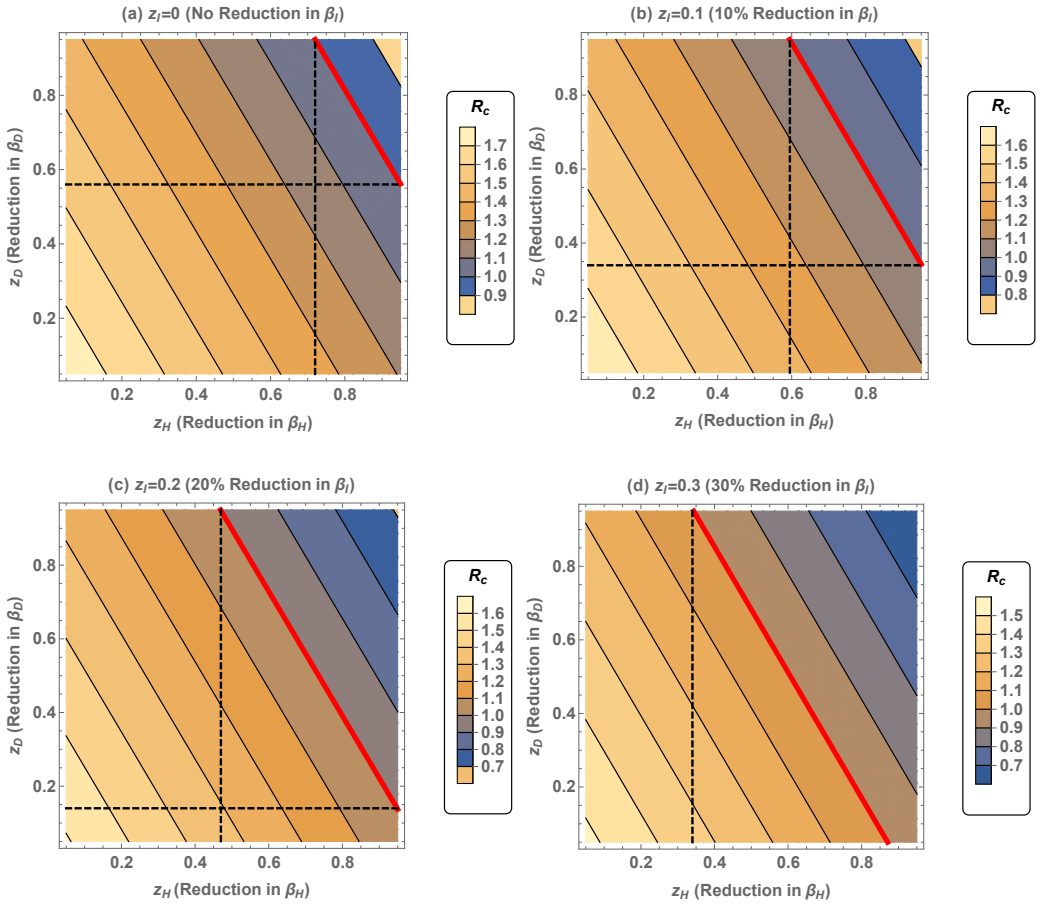

Figure 9: Contour plots showing changes in $\mathcal{R}_c$ as a function of z_H and z_D (decreases in β_H and β_D) for various levels of reduction z_I in β_I. The thick line in each plot corresponds to $\mathcal{R}_c$=1.

A probability distribution (PDF) was assigned to each parameter which described the range of possible values and the probability that they have of occurring. The PDFs were chosen based on the biology of the disease and depending on whether the parameter was estimated or obtained from existing literature. ϵ was fixed, as well as the proportions for β_H and β_D, since only β_I was estimated and they are proportional to β_I. For all the parameters, except δ, a triangular distribution was used since it is recommended for cases in which a most likely value and a range for each parameter was estimable [26]. In the case of δ, a uniform distribution was used since studies provide a wide range for this parameter. Partial rank relation coefficients (PRCC) were computed between the values of the seven parameters which identified the independent effect of each parameter on $\mathcal{R}_0$. In this study, we assume statistical independence of the input parameters.

The results are illustrated in Figure 10.

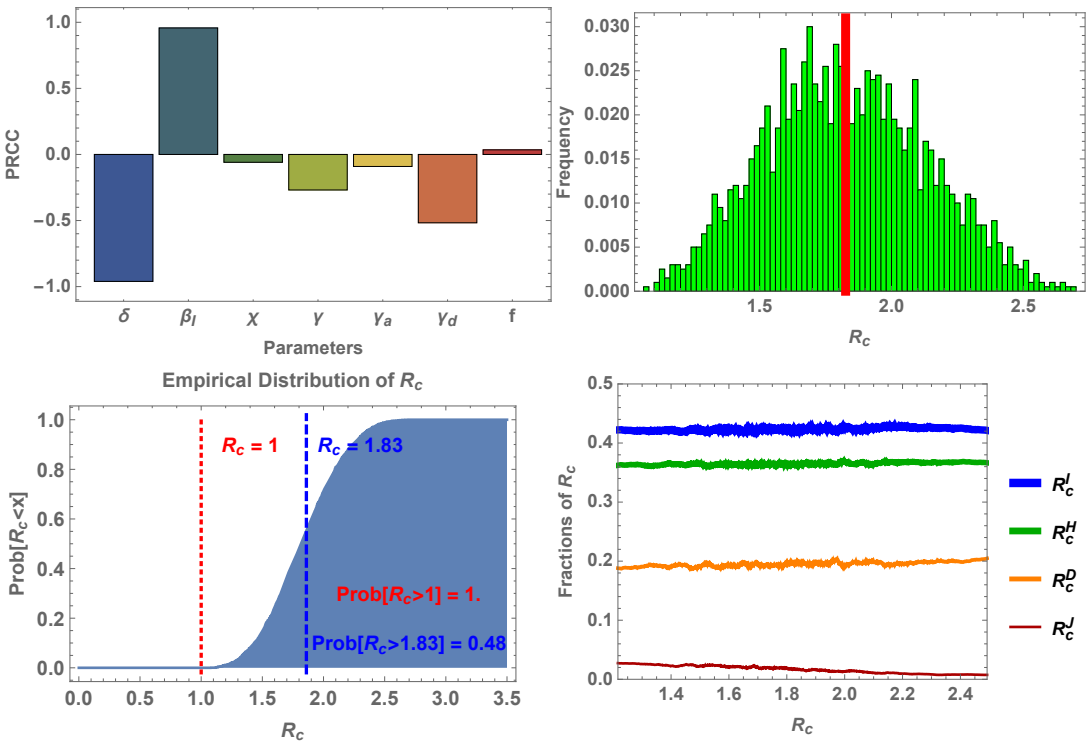

Figure 10: Sensitivity and uncertainty analyses of the basic reproduction number $\mathcal{R}_c$ with respect to model parameters. Values of the parameters are chosen using the Latin hypercube sampling method, with the ranges around the values corresponding to the case of 30% moderate infections as listed in Table 1. The plots in the top row show the PRCC values of these parameters (left) and the distribution of $\mathcal{R}_c$ (right). The bottom row shows the empirical CDF of $\mathcal{R}_c$ (left) and the contributions of $\mathcal{R}_c^i$ $(i = I, H, D, J)$ to $\mathcal{R}_c$ (right).

6.2 Sensitivity analysis of peak and final epidemic sizes

Under the control measures corresponding to the z_i $(i = I, H, D, \chi)$ in case (ii) of Table 3, deterministic simulations generate the peak and final sizes shown in Figure 4. When parameters are selected based on LHS with 1000 simulated epidemics, the distributions of the peak and final sizes are illustrated in Figure 11. The parameter ranges correspond to the case (c) in Table 2 and (ii) in Table 3, and the time to intervention is the baseline scenario (i.e., $t_c = 100$ days). We observe that, although the means for both the peak (a) and the final (b) sizes are consistent with those shown in Figure 4 (the thick solid curve), the variances are large.

6.3 Control measures and their effects on the time course

To assess the importance of various control measures for future outbreaks, we conducted a time course sensitivity analysis based on the 2014-15 Liberia outbreak. This is done again through Latin hypercube sampling of the control parameters represented by z_I, z_H, and z_D (reductions in β_I, β_H, and β_D) and

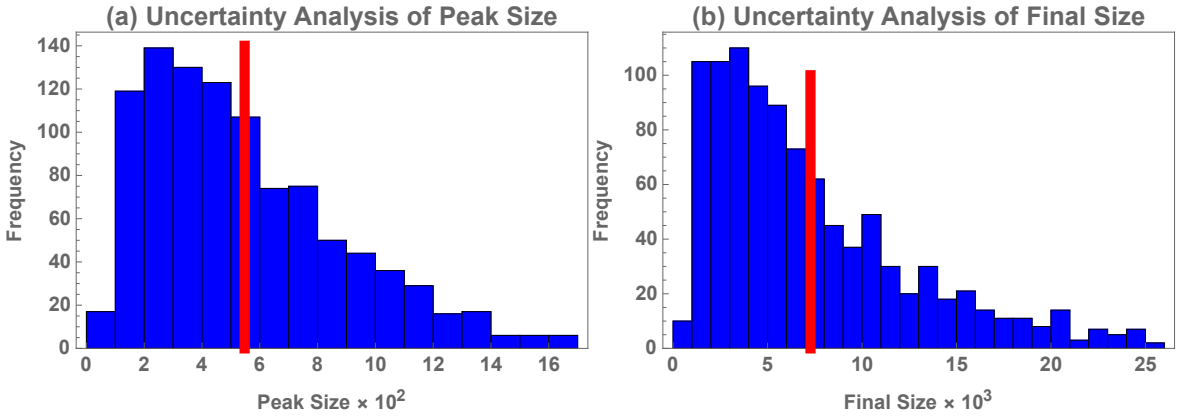

Figure 11: Similar to Figure 10(b) but results of the uncertainty analysis for the peak and final sizes. This figure illustrates distributions of the peak and final sizes of 1000 simulated epidemics with parameters selected using LHS from ranges corresponding to the case of 30% moderate infections.

the timing of intervention, denoted by T. The partial rank correlation coefficients (PRCC) are presented in Figure 12. The ranges for z_I, z_H, and z_D are same as the confidence intervals estimated in Table 3. The range for T is chosen to be between 1 week before and 1 week after the baseline scenario $t_c = 100$ (days), and the range for the reduction parameter z_χ (time from onset to hospitalization) is (0, 0.3).

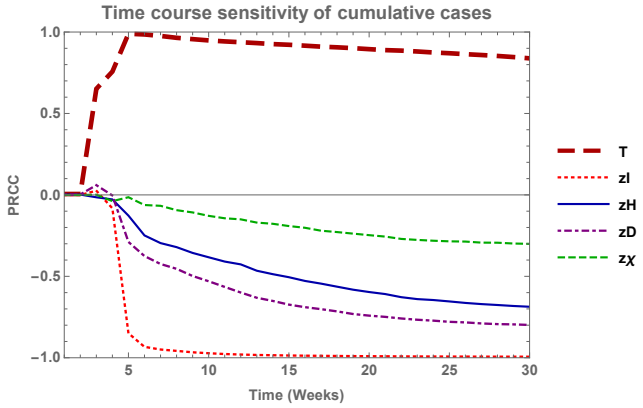

Figure 12: Time course sensitivity with respect to control parameters.

We observe that the PRCC curves of control parameters are similar and close to zero before implementation of control measures. Once control measures are implemented, the PRCC curves of different control parameters quickly approach relatively stable values. The first PRCC curve approaching 1 is the timing of control measures, which is positively correlated with cumulative cases. This is consistent with the fact that the later that control measures are implemented, the larger the outbreak. Early implementation of control measures is very important in the exponential growth phase of any outbreak. As time increases, the influence of time to intervention diminishes. All other control measures are negatively correlated, which implies that implementing these control measures mitigates the outbreak. The most influential measures are the reductions in community and hospital transmission (z_I and z_D), followed by z_H and z_χ.

7 Discussion

To investigate the impact of a spectrum of symptoms of Ebola infection, we based assumptions on biological findings about Ebola infections with moderate and severe symptoms. Those with moderately symptomatic infections from the exposed class have some viral replication, which is controlled due to strong innate immunity plus successful adaptive immunity. These individuals are not very infectious despite moderately symptomatic infections, because they have few viruses circulating within their bodies. Individuals with severe symptoms have higher viral load and therefore are more infectious than people with moderately infections. Various levels of moderately symptomatic infections are considered in our analysis based on estimates by Bower et al. [9], Bellan et al. [8] and Richardson et al.[22].

The model developed in this paper extends the Model II in [13] by explicitly including moderate infections. The formulation and its underlying assumptions are demonstrated via integro-differential equations and their reduction to ordinary differential equations in [13]. The merit of this model is that it allows the infection history to pass over even after hospitalization. This is important in determining times of recovery and death, especially when no treatment is available. The Gamma assumption also provides a realistic infectious period, and infectious individuals recover or die in the later stage of the infection, but not sooner.

The results in this paper illustrate the importance of considering infections with moderate symptoms. First, the estimated basic reproduction number $\mathcal{R}_0$ for the model with 30% moderate infections ($\delta = 0.3$) is 1.83, which is the most consistent (among the models with different δ values) with WHO's estimate independent of compartmental modeling (see Table 2). It is worth noting that our reproduction numbers are obtained by fitting our models directly to cases using maximum likelihood estimation. Alternatively, one can estimate the exponential growth rate of early cases and connect the rate to reproduction number by assuming a generation interval [29]. The estimate of $\mathcal{R}_0$ can be inflated when excluding moderate infections in the model ($\delta = 0$). However, uncertainty analysis of $\mathcal{R}_0$ of the model with 30% moderate infections could lead to reproduction numbers from 1.2 to 2.4 (see Figure 10). We show that the sensitivity of $\mathcal{R}_0$ to δ is higher than to most other parameters (see Figure 10(a)), and that the most influential components of $\mathcal{R}_0$ is $\mathcal{R}_0^I$ followed by $\mathcal{R}_0^H$ (see Figure 10(d)).

Second, the effectiveness of interventions is over-estimated when ignoring the moderate infections. For example, we demonstrate in Figures 4–6 that, although models with various δ values provide similar evaluations of the effect of control measures on the final epidemic sizes, the model with $\delta = 0$ predicts a much higher effectiveness of early intervention than models with $\delta = 0.3$. Thus, without considering moderately symptomatic infections, extra credit is given to implemented control measures. The sensitivity analysis also shows that the variances in the peak and final epidemic sizes are relatively large (Figure 11) and that the reduction in β_I (among all β_i's, $i = I, H, D, \chi$) is the most influential to the cumulative number of cases over the entire time course, while the timing of interventions diminishes (see Figure 12).

In addition, the timing of interventions is of great importance to mitigate final epidemic size. Because final size is an exponential function of the time of intervention, early interventions could significantly reduce epidemic size. An empirical regression equation linking final size and timing of interventions could be useful for policy-making.

It is necessary to stratify infections by severity of clinical symptoms in modeling. This permits reasonable estimates of the reproduction number and effectiveness of control measures, especially when infected

persons present with various symptoms. More epidemiological investigation of moderately symptomatic infections of Ebola will be helpful to estimate their fractions of the total infection and infectivity. These are crucial to more useful modeling of future outbreaks.

Acknowledgments

G. Lin would like to acknowledge the support by NSF Grants DMS-1555072 and DMS-1736364. Joan Ponce would like to acknowledge the support by NSF Grant DGE-1333468.

References

[1] 2014 Ebola Outbreak in West Africa - Reported Cases Graphs Ebola Hemorrhagic Fever, CDC. `http://www.cdc.gov/vhf/ebola/outbreaks/2014-west-africa/cumulative-cases-graphs.html`. [Online; accessed 2016-01-23].

[2] Ebola Situation Reports. `http://apps.who.int/ebola/ebola-situation-reports`. [Online; accessed 2016-02-15].

[3] WHO Statement on the 1st meeting of the IHR Emergency Committee on the 2014 Ebola outbreak in West Africa. `http://www.who.int/mediacentre/news/statements/2014/ebola-20140808/en/`. [Online; accessed 2016-02-03].

[4] Liberia Ebola Situation Report no. 58. `http://www.unicef.org/appeals/files/UNICEF_Liberia_SitRep_29_October_2014.pdf`, October 2014. [Online; accessed 2016-03-28].

[5] C. L. Althaus. Estimating the Reproduction Number of Ebola Virus (EBOV) During the 2014 Outbreak in West Africa. *PLoS Currents*, 2014.

[6] J. Audet and G. P. Kobinger. Immune evasion in ebolavirus infections. *Viral Immunol.*, 28(1):10–18, February 2015.

[7] M. Barbarossa, A. Dénes, G. Kiss, Y. Nakata, G. Röst, and Z. Vizi. Transmission Dynamics and Final Epidemic Size of Ebola Virus Disease Outbreaks with Varying Interventions. *PLoS ONE*, 10(7):e0131398, July 2015.

[8] S. E. Bellan, J. R. C. Pulliam, J. Dushoff, and L. A. Meyers. Ebola control: effect of asymptomatic infection and acquired immunity. *The Lancet*, 384(9953):1499–1500, October 2014.

[9] Hilary Bower, Sembia Johnson, Mohamed S Bangura, Alie Joshua Kamara, Osman Kamara, Saidu H Mansaray, Daniel Sesay, Cecilia Turay, Francesco Checchi, and Judith R Glynn. Exposure-specific and age-specific attack rates for ebola virus disease in ebola-affected households, sierra leone. *Emerging infectious diseases*, 22(8):1403, 2016.

[10] C. Browne, H. Gulbudak, and G. Webb. Modeling contact tracing in outbreaks with application to Ebola. *Journal of Theoretical Biology*, 384:33–49, November 2015.

[11] S. J. Chapman and A. V. S. Hill. Human genetic susceptibility to infectious disease. *Nat Rev Genet*, 13(3):175–188, March 2012.

[12] G. Chowell and H. Nishiura. Transmission dynamics and control of Ebola virus disease (EVD): a review. *BMC medicine*, 12(1):196, 2014.

[13] Z. Feng, Y. Zheng, N. Hernandez-Ceron, H. Zhao, J. Glasser, and A. Hill. Mathematical models of Ebola - Consequences of underlying assumptions. *Submitted*.

[14] Zhilan Feng, Dashun Xu, and Haiyun Zhao. Epidemiological models with non-exponentially distributed disease stages and applications to disease control. *Bulletin of mathematical biology*, 69(5):1511–1536, 2007.

[15] R. T. Heffernan, B. Pambo, R. J. Hatchett, P. A. Leman, R. Swanepoel, and R. W. Ryder. Low Seroprevalence of IgG Antibodies to Ebola Virus in an Epidemic Zone: Ogooué-Ivindo Region, Northeastern Gabon, 1997. *J Infect Dis.*, 191(6):964–968, March 2005.

[16] A. Khan, M. Naveed, M. Dur-e Ahmad, and M. Imran. Estimating the basic reproductive ratio for the Ebola outbreak in Liberia and Sierra Leone. *Infect Dis Poverty*, 4, February 2015.

[17] J. Legrand, R. F. Grais, P. Y. Boelle, A. J. Valleron, and A. Flahault. Understanding the dynamics of Ebola epidemics. *Epidemiol. Infect.*, 135(4):610–621, May 2007.

[18] E. M. Leroy, S. Baize, V. E. Volchkov, S. P. Fisher-Hoch, M-C. Georges-Courbot, J. Lansoud-Soukate, M. Capron, P. Debré, A. J. Georges, and J. B. McCormick. Human asymptomatic Ebola infection and strong inflammatory response. *The Lancet*, 355(9222):2210–2215, June 2000.

[19] J. A. Lewnard, M. L. Ndeffo Mbah, J. A. Alfaro-Murillo, F. L. Altice, L. Bawo, T. G. Nyenswah, and A. P. Galvani. Dynamics and control of Ebola virus transmission in Montserrado, Liberia: a mathematical modelling analysis. *The Lancet Infectious Diseases*, 14(12):1189–1195, December 2014.

[20] A. Pandey, K. E. Atkins, J. Medlock, N. Wenzel, J. P. Townsend, J. E. Childs, T. G. Nyenswah, M. L. Ndeffo-Mbah, and A. P. Galvani. Strategies for containing Ebola in West Africa. *Science*, 346(6212):991–995, November 2014.

[21] A. L. Rasmussen, A. Okumura, M. T. Ferris, R. Green, F. Feldmann, S. M. Kelly, D. P. Scott, D. Safronetz, E. Haddock, R. LaCasse, M. J. Thomas, P. Sova, V. S. Carter, J. M. Weiss, D. R. Miller, G. D. Shaw, M. J. Korth, M. T. Heise, R. S. Baric, F. Villena, H. Feldmann, and M. G. Katze. Host genetic diversity enables Ebola hemorrhagic fever pathogenesis and resistance. *Science*, 346(6212):987–991, November 2014.

[22] Eugene T Richardson, J Daniel Kelly, Mohamed Bailor Barrie, Annelies W Mesman, Sahr Karku, Komba Quiwa, Regan H Marsh, Songor Koedoyoma, Fodei Daboh, Kathryn P Barron, et al. Minimally symptomatic infection in an ebola ?hotspot?: a cross-sectional serosurvey. *PLoS neglected tropical diseases*, 10(11):e0005087, 2016.

[23] C. M. Rivers, E. T. Lofgren, M. Marathe, S. Eubank, and B. L. Lewis. Modeling the Impact of Interventions on an Epidemic of Ebola in Sierra Leone and Liberia. *PLoS Curr*, 6, November 2014.

[24] T. H. Roels, A. S. Bloom, J. Buffington, G. L. Muhungu, W. R. Mac Kenzie, A. S. Khan, R. Ndambi, D. L. Noah, H. R. Rolka, C. J. Peters, and T. G. Ksiazek. Ebola Hemorrhagic Fever, Kikwit, Democratic Republic of the Congo, 1995: Risk Factors for Patients without a Reported Exposure. *J Infect Dis.*, 179(Supplement 1):S92–S97, February 1999.

[25] A. Sanchez, K. E. Wagoner, and P. E. Rollin. Sequence-based human leukocyte antigen-B typing of patients infected with Ebola virus in Uganda in 2000: identification of alleles associated with fatal and nonfatal disease outcomes. *J. Infect. Dis.*, 196 Suppl 2:S329–336, November 2007.

[26] Gordon L Swartzman and Stephen P Kaluzny. *Ecological simulation primer*. 1987.

[27] M. D. Van Kerkhove, A. I. Bento, H. L. Mills, N. M. Ferguson, and C. A. Donnelly. A review of epidemiological parameters from Ebola outbreaks to inform early public health decision-making. *Scientific Data*, 2:150019, May 2015.

[28] G. Webb, C. Browne, X. Huo, O. Seydi, M. Seydi, and P. Magal. A Model of the 2014 Ebola Epidemic in West Africa with Contact Tracing. *PLoS Currents*, 2015.

[29] Dushoff J. Weitz, J. S. Modeling Post-death Transmission of Ebola: Challenges for Inference and Opportunities for Control. *Scientific Reports*, 5:8751, March 2015.

[30] WHO Ebola Response Team. Ebola Virus Disease in West Africa — The First 9 Months of the Epidemic and Forward Projections. *New England Journal of Medicine*, 371(16):1481–1495, October 2014.

[31] G. Wong, G. P. Kobinger, and X. Qiu. Characterization of host immune responses in Ebola virus infections. *Expert Review of Clinical Immunology*, 10(6):781–790, June 2014.

[32] C. A. Zampieri, N. J. Sullivan, and G. J. Nabel. Immunopathology of highly virulent pathogens: insights from Ebola virus. *Nat. Immunol.*, 8(11):1159–1164, November 2007.